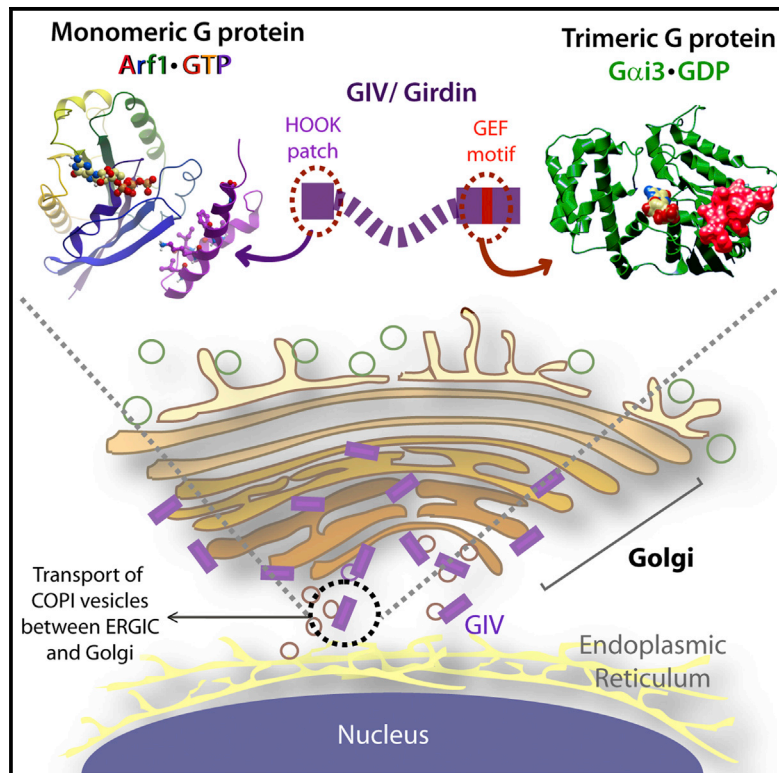# Developmental Cell

Activation of Gαi at the Golgi by GIV/Girdin Imposes Finiteness in Arf1 Signaling

Graphical Abstract

Authors

I-Chung Lo, Vijay Gupta, ...,
Marilyn G. Farquhar, Pradipta Ghosh

Correspondence

mfarquhar@ucsd.edu (M.G.F.),
prghosh@ucsd.edu (P.G.)

In Brief

During canonical G protein signaling, G protein-coupled receptors (GPCRs) function as guanine exchange factors (GEFs) at the plasma membrane. Lo et al. show that GIV, a non-receptor GEF, activates Gi proteins at the Golgi and, via modulation of Arf1 signaling, regulates vesicle trafficking and Golgi organization.

Highlights

- Arf1·GTP directly binds and recruits GIV to COPI vesicles via GIV's HOOK domain

- GIV activates trimeric Gi at the Golgi and releases Gβγ, which terminates Arf1·GTP

- Finiteness of Arf1 activity imposed by GIV maintains Golgi structure and functions

- GIV is a platform for crosstalk between trimeric G proteins and monomeric Arf1 GTPase

CrossMark

CellPress

Article

Cell Press

Activation of Gαi at the Golgi by GIV/Girdin Imposes Finiteness in Arf1 Signaling

I-Chung Lo,[1] Vijay Gupta,[1] Krishna K. Midde,[2] Vanessa Taupin,[1] Inmaculada Lopez-Sanchez,[2] Irina Kufareva,[3] Ruben Abagyan,[3] Paul A. Randazzo,[4] Marilyn G. Farquhar,[1,*] and Pradipta Ghosh[2,*]

[1]Departments of Cellular and Molecular Medicine, University of California, San Diego, La Jolla, CA 92093, USA
[2]Department of Medicine, University of California, San Diego, La Jolla, CA 92093, USA
[3]Skaggs School of Pharmacy and Pharmaceutical Sciences, University of California, San Diego, La Jolla, CA 92093, USA
[4]Laboratory of Cellular and Molecular Biology, Center for Cancer Research, National Cancer Institute, Bethesda, MD 20892, USA
*Correspondence: mfarquhar@ucsd.edu (M.G.F.), prghosh@ucsd.edu (P.G.)
http://dx.doi.org/10.1016/j.devcel.2015.02.009

SUMMARY

A long-held tenet of heterotrimeric G protein signal transduction is that it is triggered by G protein-coupled receptors (GPCRs) at the PM. Here, we demonstrate that Gi is activated in the Golgi by GIV/Girdin, a non-receptor guanine-nucleotide exchange factor (GEF). GIV-dependent activation of Gi at the Golgi maintains the finiteness of the cyclical activation of ADP-ribosylation factor 1 (Arf1), a fundamental step in vesicle traffic in all eukaryotes. Several interactions with other major components of Golgi trafficking—e.g., active Arf1, its regulator, ArfGAP2/3, and the adaptor protein β-COP—enable GIV to coordinately regulate Arf1 signaling. When the GIV-Gαi pathway is selectively inhibited, levels of GTP-bound Arf1 are elevated and protein transport along the secretory pathway is delayed. These findings define a paradigm in non-canonical G protein signaling at the Golgi, which places GIV-GEF at the crossroads between signals gated by the trimeric G proteins and the Arf family of monomeric GTPases.

INTRODUCTION

Canonical G protein signaling is believed to emanate exclusively from the plasma membrane (PM) (Gilman, 1987), triggered by ligand-bound G protein coupled receptors (GPCRs) that serve as guanine nucleotide exchange factors (GEFs). However, gathering evidence indicates that trimeric G proteins are also activated independent of GPCRs at different intracellular organelles and that such activation plays crucial roles in cells (Hewavitharana and Wedegaertner, 2012). The Golgi complex has emerged as a major hub for such intracellular signaling because it contains G proteins and a plethora of modulators of G protein signaling; e.g., kinases, phosphatases, and phospholipases (Cancino and Luini, 2013).

Heterotrimeric G proteins were detected in the Golgi over two decades ago (Barr et al., 1992; Stow et al., 1991), and numerous studies have provided clues that they may regulate membrane traffic and maintain the structural integrity of the Golgi (Cancino and Luini, 2013). However, the concept of G protein activation at

the Golgi and the potential impact of such activation are met with skepticism, primarily due to the lack of direct proof of G protein activation. We recently discovered a non-receptor guanidine exchange factor (GEF) for Gαi, GIV (Garcia-Marcos et al., 2009) (also known as Girdin), a multi-modular signal transducer that binds phosphatidylinositol 4-phosphate (PI(4)P; see Enomoto et al., 2005) and primarily localizes to the Golgi on COPI vesicles (Le-Niculescu et al., 2005). Activation of Gαi via GIV's GEF motif has been implicated in the regulation of diverse cellular processes including cell migration, endosomal trafficking, and autophagosome maturation (Garcia-Marcos et al., 2015). Because GIV and trimeric G proteins localize on Golgi membranes and because GIV is a bona fide GEF for Gαi (Garcia-Marcos et al., 2009), we investigated whether GIV-GEF activates Gαi in the Golgi. We provide direct evidence that activation of Gαi by GIV in the Golgi affects two fundamental functions of the Golgi; i.e., vesicle trafficking and the structural organization of the Golgi stacks, both via modulation of Arf1 signaling. These findings break the impasse on whether Gαi is functionally active in the Golgi.

RESULTS AND DISCUSSION

GIV Binds and Activates Gαi in the Golgi Complex

We previously showed that Gαi3 is found in both the Golgi region and at the PM (Weiss et al., 2001), and that GIV colocalizes with Gαi3 at both sites (Le-Niculescu et al., 2005). By double immunostaining, GIV and Gαi3 show a perinuclear, Golgi-like distribution, and colocalize with β-COP, one of the COPI coatomer subunits (Figure S1A). To determine if GIV and Gαi3 interact in the Golgi, we performed proximity ligation assays (PLA) (Söderberg et al., 2006) to detect in situ GIV-Gαi3 complexes in COS7 cells transfected with Gαi3 internally tagged with yellow fluorescent protein (YFP) (Gαi3-YFP). PLA signals were detected between endogenous GIV and Gαi3-YFP in the Golgi region (Figure 1A), indicating that they interact (i.e., the maximum distance between the two is ≤30–40 nanometers; see Söderberg et al., 2006). However, GIV did not interact with the Gαi3-YFP W258F mutant (Figure 1A), henceforth referred to as Gαi3-WF, which cannot bind or be activated by GIV, but interacts with Gβγ, GPCRs, and Gαi regulators (Garcia-Marcos et al., 2010) and localizes to the Golgi similar to Gαi3-wild-type (WT) (Figure S1B). Next, we asked if the Gαi that resides at the Golgi is active and if such activation requires GIV. To this end, we used a previously
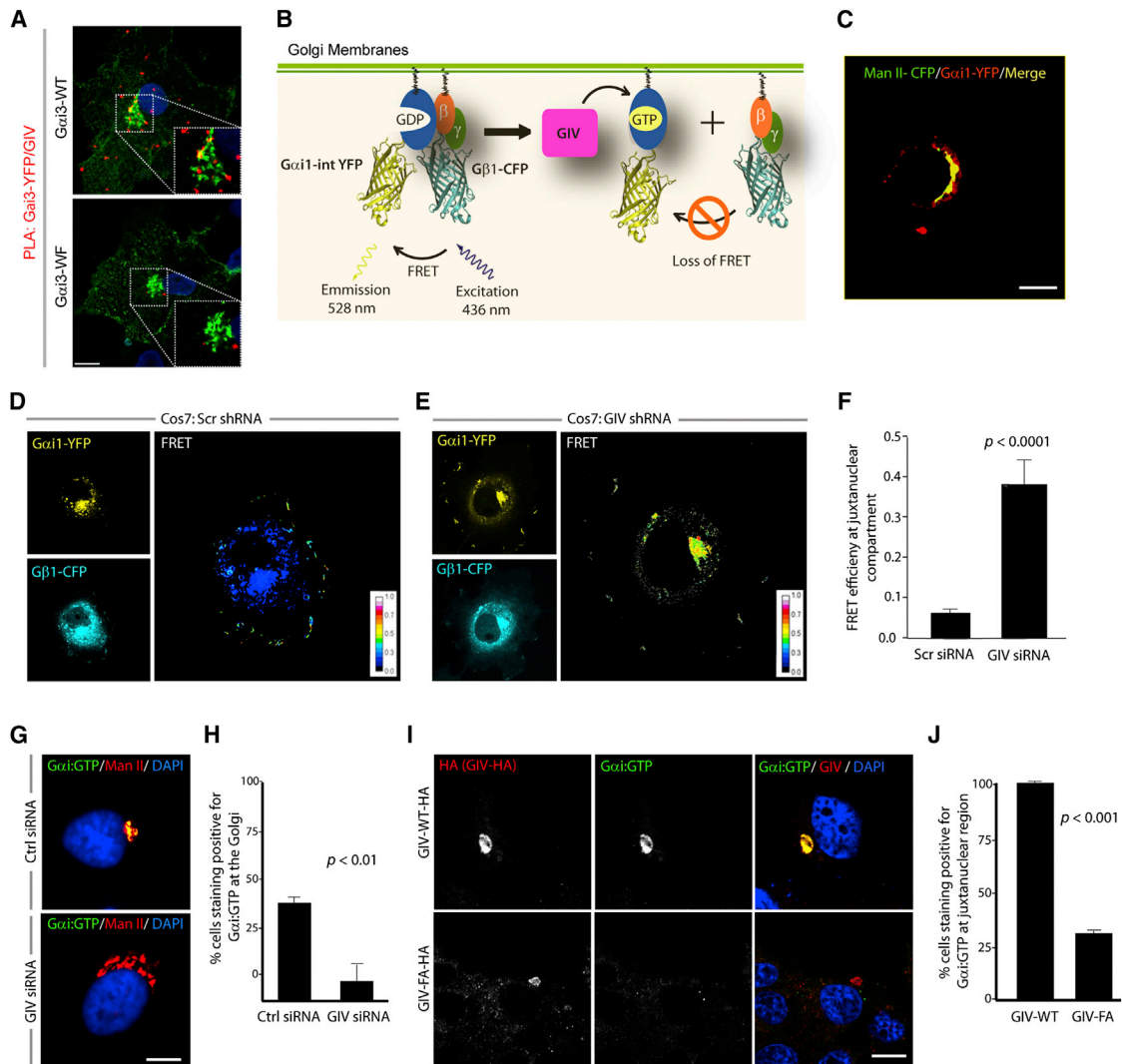
CrossMark

Figure 1. GIV Activates Gαi at the Golgi via Its GEF Motif

(A) COS7 cells transfected with YFP-tagged Gαi3-WT or the Gαi3-WF mutant were analyzed for interaction between endogenous GIV and Gαi3-YFP by in situ PLA using mouse anti-GFP and rabbit anti-GIV antibodies. Red spots indicate the presence of interaction. Insets show the Golgi region at higher magnification (white dashed box). The scale bar represents 10 μm.

(B) Schematic for the Gαi1-YFP and Gβ1-CFP constructs used as paired FRET probes in (D and E). FRET indicates the presence of inactive trimer, whereas activation of Gi is associated with loss of FRET.

(C) COS7 cells expressing Gαi1-YFP (pseudo-colored green) and Man II-CFP (pseudo-colored red) were fixed and analyzed by confocal microscopy. A high degree of colocalization (yellow pixels) indicates that the Gαi1-YFP predominantly localizes on the Golgi.

(D and E) Control (Scr shRNA) and GIV-depleted (GIV shRNA) COS7 cells (see also Figure S1C) were cotransfected with Gαi1-YFP, Gβ1-CFP, and Gγ2 (untagged) and live cells were analyzed by FRET imaging at steady-state, in the presence of 10% serum. Representative freeze-frame YFP, CFP, and FRET images are shown. FRET image panels display intensities of acceptor emission due to efficient energy transfer in each pixel.

(F) Bar graph displays FRET efficiency (y axis). FRET at the Golgi is strong in GIV-depleted cells (E); FRET efficiency = 0.37 ± 0.06, but minimal in controls (D); FRET efficiency = 0.061 ± 0.01. Results are expressed as mean ± SD. Data represent five ROIs analyzed over the pixels corresponding to the Golgi of 3–5 cells from five independent experiments.

(G) Control (Ctrl siRNA) and GIV-depleted (GIV siRNA) COS7 cells (see also Figure S1D) maintained in 10% serum were fixed and stained for active Gαi (green; anti-Gαi:GTP mAb) and Man II (red) and analyzed by confocal microscopy. Activation of Gαi was detected frequently in control, but not in GIV-depleted cells. When detected, active Gαi colocalizes with Man II (yellow pixels in upper panel).

(H) Bar graph displays % cells that stain positive for active Gαi (y axis) in control and GIV-depleted cells analyzed in (G).

(I) Active Gαi is detected frequently in cells expressing GIV-WT (upper), but not in those expressing GIV-FA (lower). When detected, active Gαi colocalizes with GIV-HA (yellow pixels in merged panel). COS7 cells expressing HA-tagged GIV-WT or GIV-FA were fixed and stained for GIV (red; anti-HA mAb) and active Gαi (green; anti-Gαi:GTP mAb) and analyzed by confocal microscopy.

(J) Bar graph displays % cells expressing GIV-HA (WT or FA) that stain positive for active Gαi (y axis) in (I).

well-established Förster resonance energy transfer (FRET)-based assay in living cells (Gibson and Gilman, 2006) in which dissociation of Gαi1-YFP and CFP-Gβ1γ2 (low FRET) is used as a surrogate marker for "activation" of Gi (Figure 1B). We found that Gαi1-YFP localized to the Golgi (Figure 1C), but showed minimal FRET with CFP-Gβ1γ2 heterodimers in that region (0.061 ± 0.01; Figure 1D) in control COS7 cells, indicative of the presence of active G proteins at the Golgi. By contrast, in GIV-depleted COS7 cells (Figure S1C) FRET efficiency was significantly higher at the Golgi region (∼6-fold) (0.37 ± 0.06; Figures 1E and 1F), indicating that in the absence of GIV, Gαi stays complexed with Gβγ as inactive heterotrimers at the Golgi. Using anti-Gαi:guanosine-5′-triphosphate (GTP) mAb, which specifically recognizes the GTP-bound active conformation of the Gαi (1/2/3) proteins (Lane et al., 2008), we further confirmed that active Gαi was frequently detected at the Golgi in control cells, where it colocalized with Man II, but not detected in GIV-depleted cells (Figures 1G, 1H, and S1D). As anticipated, we found that the GEF motif of GIV is essential for activation of Gαi at the Golgi because active Gαi was frequently detected at the perinuclear Golgi region in COS7 cells expressing WT GIV (GIV-WT), but not in cells expressing a GEF-deficient GIV mutant, GIV-FA that cannot bind or activate Gαi (Garcia-Marcos et al., 2009) (Figures 1I and 1J). These results demonstrate that Gαi is active in the Golgi and that such activation requires GIV.

GIV Interacts with β-COP on COPI Vesicles

Next, we asked with which population of Golgi-derived vesicles GIV and Gαi3 are associated. Previously, we showed that GIV colocalizes with COPI vesicles and Golgi membranes by immunofluorescence and immunogold electron microscopy labeling (Le-Niculescu et al., 2005). First, we prepared a crude membrane fraction (100,000 × g pellet) from COS7 cells (Figure S2A) and immunoisolated COPI membranes from this fraction using CM1A10, an antibody that recognizes the assembled COPI coat (coatomer) (Palmer et al., 1993), and verified that both GIV and Gαi3 were enriched on COPI-coated membranes (Figure 2A). Next, we asked if GIV interacts with COPI coat proteins in cells. We detected PLA signals between endogenous GIV and COPI-coated membranes in the Golgi as marked by expressing YFP-tagged β-Galactosyl transferase (GalT), as well as scattered throughout the cytoplasm (Figures 2B, S2B, and S2C left). This distribution of PLA signal indicates that GIV associates with COPI at the Golgi and the peripheral ERGIC, one of the major organelles where COPI-coated vesicles are found besides the Golgi (Oprins et al., 1993). Pull-down assays from HeLa cells expressing glutathione S-transferases (GST)-tagged full-length GIV showed that β-COP, a component of the heptameric COPI coat complex, as well as Gαi3, used as a positive control, bound to GIV (Figure S2D). Finally, we found that GIV coimmunoprecipitates with β-COP, but such interaction is lost when cells are incubated with 5 μg/ml brefeldin (BFA), a fungal metabolite that prevents the binding of COPI coats to membranes and releases β-COP into the cytosol (Figure 2C). BFA treatment also significantly reduced (by ∼62%) the signals detected by in situ PLA between GIV and COPI vesicles (Figure S2C, right), indicating that GIV and β-COP interact only when the latter can be recruited to membranes. No such interaction was seen between GIV and SEC13, a component of

COPII vesicle coats (Figure S2E). Together these data reveal that GIV forms a complex specifically with COPI coatomer on membranes.

GIV and Its GEF Function Are Required for Uncoating of COPI Vesicles

Next, we asked if depletion of GIV alters the association of COPI with membranes. Membrane-cytosol fractionation studies showed that compared to controls, membrane-associated β-COP was increased by ∼42% in GIV-depleted cells (Figures 2D and 2E). When we carried out similar assays in GIV-depleted cells that were infected with adenovirus containing short interfering (si)RNA-resistant GIV-WT or the GIV-FA mutant that does not bind or activate Gαi3 (Garcia-Marcos et al., 2009), we found that membrane-associated β-COP was increased by ∼37% in cells expressing inactive GIV-FA compared to active GIV-WT (Figures 2F and 2G). These findings indicate that the GEF motif, via which GIV activates Gαi3, is essential to reduce membrane-association of β-COP.

Next, we explored the effect of GIV depletion on the distribution of COPI vesicles by immunofluorescence. In cells treated with control siRNA, β-COP was mostly associated with Golgi membranes and a few COPI vesicles concentrated in and around the Golgi region, whereas in GIV-depleted cells, abundant COPI vesicles were seen dispersed peripherally throughout the cytoplasm (Figure 2H). Quantification revealed that the peripheral pool of vesicles was increased ∼2.6-fold after GIV depletion (Figure 2I). A similar ∼2-fold increase in the peripheral pool of COPI vesicles was also seen in cells expressing the GEF-deficient GIV-FA mutant when compared to those expressing GIV-WT (Figures 2J and S2F), indicating that GIV and its GEF motif are essential for normal distribution of COPI vesicles. To corroborate accumulation of COPI vesicles after GIV depletion, we prepared enriched vesicle fractions by differential centrifugation and found that β-COP was increased ∼2-fold in vesicle fractions (100,000 × g pellet fraction, [P3]) obtained from GIV-depleted cells (Figures 2K and 2L), which is consistent with the immunofluorescence findings (Figures 2H and 2I), indicating that COPI-coated vesicles accumulate after GIV depletion. GM130, used as a Golgi marker, was concentrated in the Golgi enriched fraction (15,000 × g pellet, P2) and was not detected in the enriched vesicle fraction (Figure 2K), indicating that Golgi membranes were not present in this fraction and thus not vesiculated during homogenization. Furthermore, we confirmed by immunoblotting that the observed changes in distribution of β-COP were not due to changes in the total levels of the protein (Figures S2G and S2H). The accumulation of budded vesicles with β-COP coats in the cell periphery (Figures 2H and 2I), together with the shift in β-COP from the cytosol to membrane fractions (Figures 2D and 2E), point to a defect in uncoating of COPI vesicles in the absence of GIV, and suggest a role for GIV in facilitating the uncoating of COPI vesicles. The results with the GEF deficient GIV-FA mutant imply that activation of Gαi3 by GIV is required for uncoating.

Next, we analyzed the nature of the compartments where the COPI coat accumulated. Immunofluorescence labeling showed that in control cells, there were very few β-COP-stained puncta (COPI vesicles) in the cell periphery (away from the Golgi; Figure S3A), showing limited colocalization with or proximity to
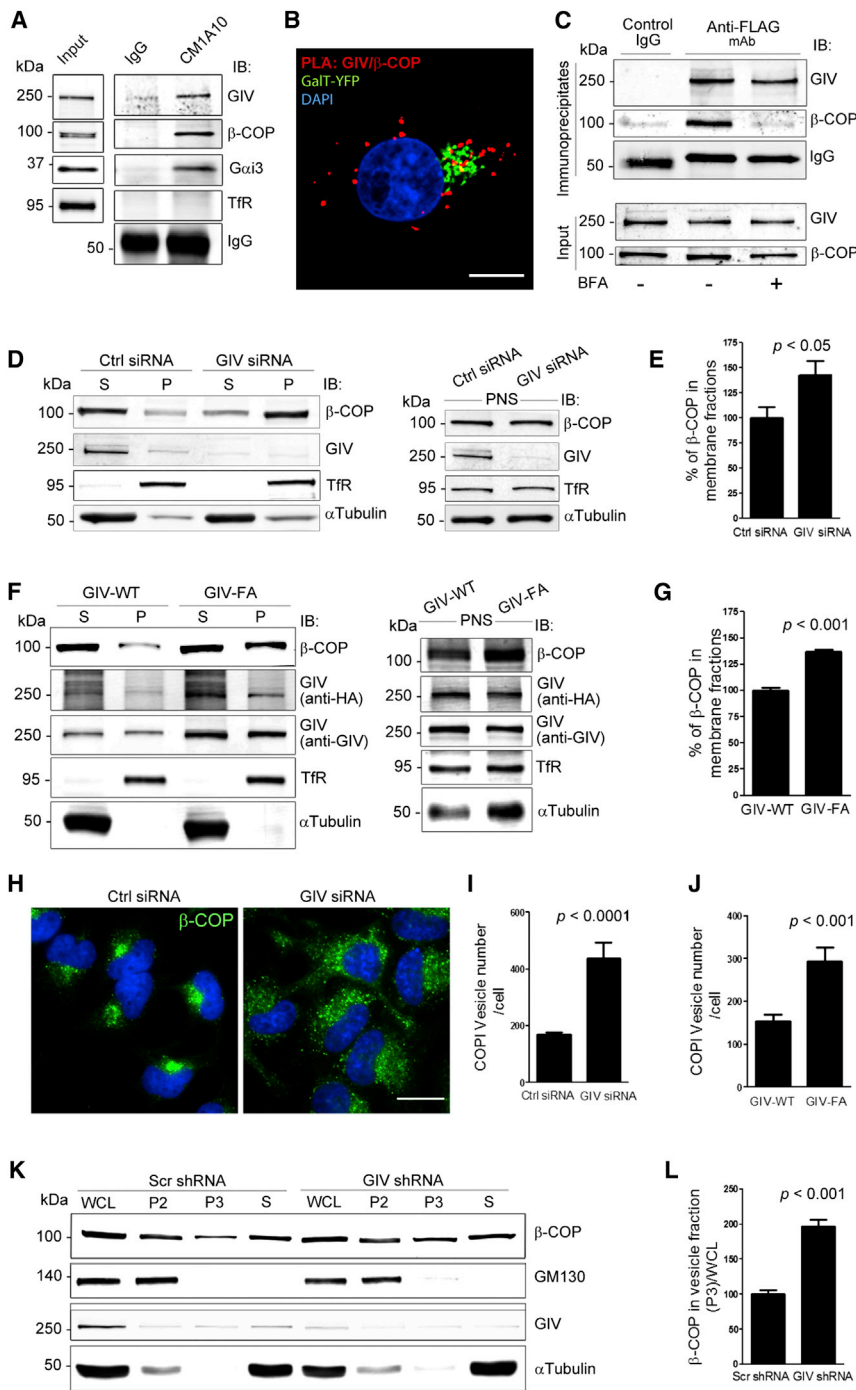
Figure 2. GIV Associates with COPI Vesicles and Is Required for Uncoating of COPI Vesicles

(A) COPI membranes were immunoisolated from a crude membrane (100,000 × g pellet; see Figure S2A) fraction prepared from COS7 cells using mAb CM1A10 (which recognizes coatomer), and bound immune complexes were analyzed for GIV, β-COP, Gαi3, and transferrin receptor (TfR, a negative control) by immunoblotting (IB).

(B) HeLa cells expressing GalT-YFP (Golgi marker, pseudocolored green) were fixed and analyzed for interactions between GIV and β-COP by in situ PLA (red). Nuclei = DAPI (blue). The scale bar represents 10 μm. Negative control (S2B) showed no signal.

(C) HeLa cells expressing GIV-FLAG were treated or not with 5 μg/ml BFA for 30 min prior to lysis. Equal aliquots of lysates were immunoprecipitated with anti-FLAG mAb and immune complexes were analyzed for β-COP by immunoblotting.

(D) Membrane (P, 100,000 × g pellet) and cytosolic (S, 100,000 × g supernatant) fractions (left panel) were prepared from post-nuclear supernatants (PNS, right panel) of control (Ctrl siRNA) or GIV-depleted (GIV siRNA) COS7 cells and analyzed for the indicated proteins by immunoblotting.

(E) Bar graphs display the relative abundance of β-COP in membrane fractions in (D), derived from the equation $[(P) / (S + P)] \times 100$. Data were normalized to control and expressed as % changes. Results are expressed as mean ± SEM.

(F) GIV-depleted cells were treated with adenovirus containing RNAi-resistant GIV-WT or GIV-FA. Homogenates of these cells were used to prepare membrane and cytosolic fractions as in (D) and analyzed by immunoblotting.

(G) Bar graphs display the relative abundance of β-COP in membrane fractions in (F).

(H) Control (Ctrl siRNA) or GIV-depleted (GIV siRNA) HeLa cells were prepermeabilized with 0.1% Saponin (to release cytosolic β-COP), stained for β-COP (green) and the nucleus (DAPI, blue), and analyzed by confocal microscopy. The scale bar represents 10 μm.

(I) Bar graphs display the number of COPI vesicles per cell in (H), as determined by 3D-reconstruction using Imaris software (n = 3; mean ± SEM; >20 cells/experiment).

(J) Bar graphs display the number of COPI vesicles in adeno-GIV-WT-HA or -GIV-FA-HA infected cells (see Figure S2F) that were analyzed exactly as in (H and I) (n = 3; mean ± SEM; >10 cells/experiment/condition).
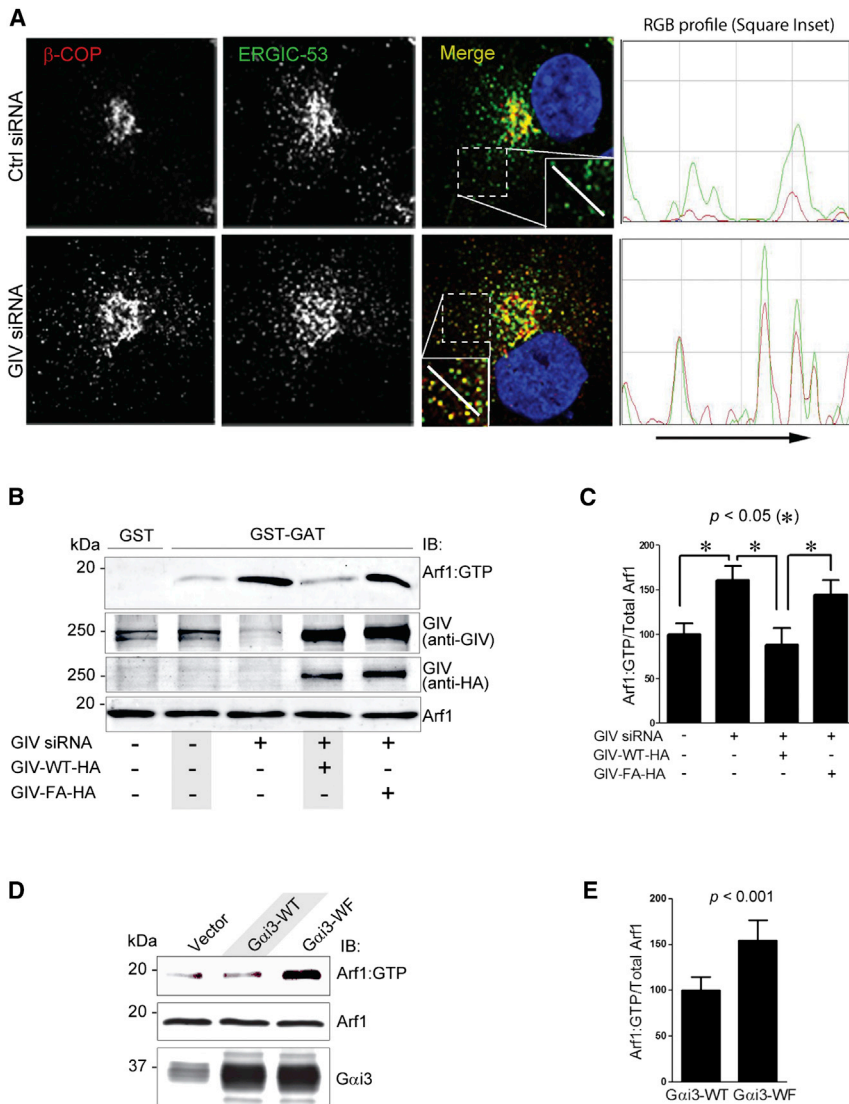
(K) Whole cell lysates (WCL) of control (Scr shRNA) or GIV-depleted (GIV shRNA) cells were subjected to differential centrifugation to obtain a 15,000 × g

(P2) fraction enriched in Golgi membranes, a 100,000 × g (P3) fraction containing COPI vesicles, and a cytosolic fraction (S, 100,000 × g supernatant). Fractions were analyzed for GIV, β-COP, and GM130 (Golgi marker) by immunoblotting.

(L) Bar graphs display the quantification of β-COP in P3 fractions normalized to WCL. Increased membrane-association of β-COP as determined by membrane-cytosol fractionation or increased peripheral vesicular staining of β-COP we observe in GIV-depleted cells (D, E, H, and I) or in cells expressing GIV-FA (F, G, and J) is not due to changes in absolute cellular levels of β-COP (see Figures S2G and S2H).

ERGIC-53, an ER/Golgi intermediate compartment marker protein (Figures 3A and S3B). By contrast, in GIV-depleted cells, numerous punctate β-COP-stained vesicles were seen in the cell periphery (Figure S3A), frequently colocalizing with or in close proximity to clusters of tubulo-vesicular ERGIC structures (Figures 3A and S3B). Because such colocalization was previously reported (Saitoh et al., 2009) in cells with higher levels of active Arf1, these results suggest that depletion of GIV or

Figure 3. Activation of Gαi by GIV Terminates Arf1 Signaling

(A) Depletion of GIV promotes accumulation of COPI vesicles in the ER-Golgi intermediate compartment (ERGIC). Left, control (Ctrl siRNA, upper panel) or GIV-depleted (GIV siRNA, lower panel). HeLa cells were fixed and stained for β-COP (red) and ERGIC-53 (green). Merged panels display the overlay of β-COP (red) and ERGIC-53 (green) panels. Insets on merge panels viewed at higher magnification show limited colocalization of ERGIC-53 with β-COP in the *cis*-Golgi in control cells and that ERGIC-53 is also found in vesicles scattered throughout the cytoplasm, which do not stain for β-COP. In GIV-depleted cells there is increased colocalization between β-COP and ERGIC-53 and these vesicular structures that co-stain for both β-COP and ERGIC-53 are more dispersed. The white line in the insets indicates the pixels used for the red green blue (RGB) profile plots shown (see Experimental Procedures). The scale bar represents 10 μm. Right, RGB profiles of ERGIC-53 (green) and β-COP (red) corresponding to lines in merge of (A) as shown in insets.

(B) COS7 cells were treated with control (-) or GIV siRNA (+) and adenoviral vectors expressing siRNA-resistant GIV-WT or GIV-FA as indicated. Equal aliquots of lysates (bottom panels, 5% input) were analyzed for Arf1·GTP by carrying out GST pull-down assays with GST-GGA3. Bound proteins (top panel) were analyzed for active Arf1 by immunoblotting.

(C) Bar graph displays the band densitometry quantification of Arf1·GTP (bound)/total Arf1 (inputs) in (B). Data were normalized to control and expressed as % changes. Results are expressed as mean ± SEM.

(D) COS7 cells expressing Gαi3-WT, Gαi3-WF mutant, or control vector were analyzed for levels of Arf1·GTP as in (B).

(E) Bar graph displays the band densitometry quantification of Arf1·GTP (bound)/total Arf1 (inputs) in (D). Results are expressed as mean ± SEM.

inhibition of GIV's GEF activity may perturb uncoating of COPI vesicles via an underlying fundamental defect in the regulation of Arf1.

GIV Suppresses the Levels of Arf1·GTP via Its Ability to Activate Gαi

To determine if GIV or its GEF function modulate Arf1 activity in cells, we used the previously validated pull-down assay with a GST-GAT domain of GGA3, which selectively binds the active GTP-bound pool of Arf1 (Cohen and Donaldson, 2010). We found that compared to control cells, the levels of Arf1·GTP were increased ∼60% in GIV-depleted cells (Figures 3B and 3C). This increase was effectively reversed to normal levels by the expression of siRNA-resistant hemagglutinin (HA)-tagged GIV-WT, but not by the GEF deficient GIV-FA mutant (Figures 3B and 3C). These findings indicate that GIV is required for downregulation of Arf1·GTP, and that GIV's GEF function (which activates Gαi) is required for this effect.

To confirm that activation of Gαi3 by GIV regulates the levels of active Arf1, we transfected cells with WT Gαi3 or the W258F mutant of Gαi3 that cannot be activated by GIV and assessed the level of Arf1·GTP. We found that Arf1·GTP was increased by ∼70% in the cells expressing Gαi3-W258F compared to Gαi3-WT (Figures 3D and 3E), indicating that activation of Gαi3 by GIV is essential for downregulation of Arf1 signaling, and that inhibition of the GIV-Gαi axis results in increased active Arf1.

GIV and Its GEF Function Regulate ER-Golgi Vesicle Transport

To determine if accumulation of COPI vesicles and increased active Arf1 in GIV-depleted cells also affects protein trafficking along the secretory pathway, we examined the transport of vesicular stomatitis virus G protein (VSVG) from the ER to the PM using the well-characterized GFP-tagged VSVG-tsO45 mutant. This mutant VSVG is retained in the ER at 40°C and moves out of the ER and passes through the Golgi to the PM when shifted to 32°C (Gallione and Rose, 1985). Surface
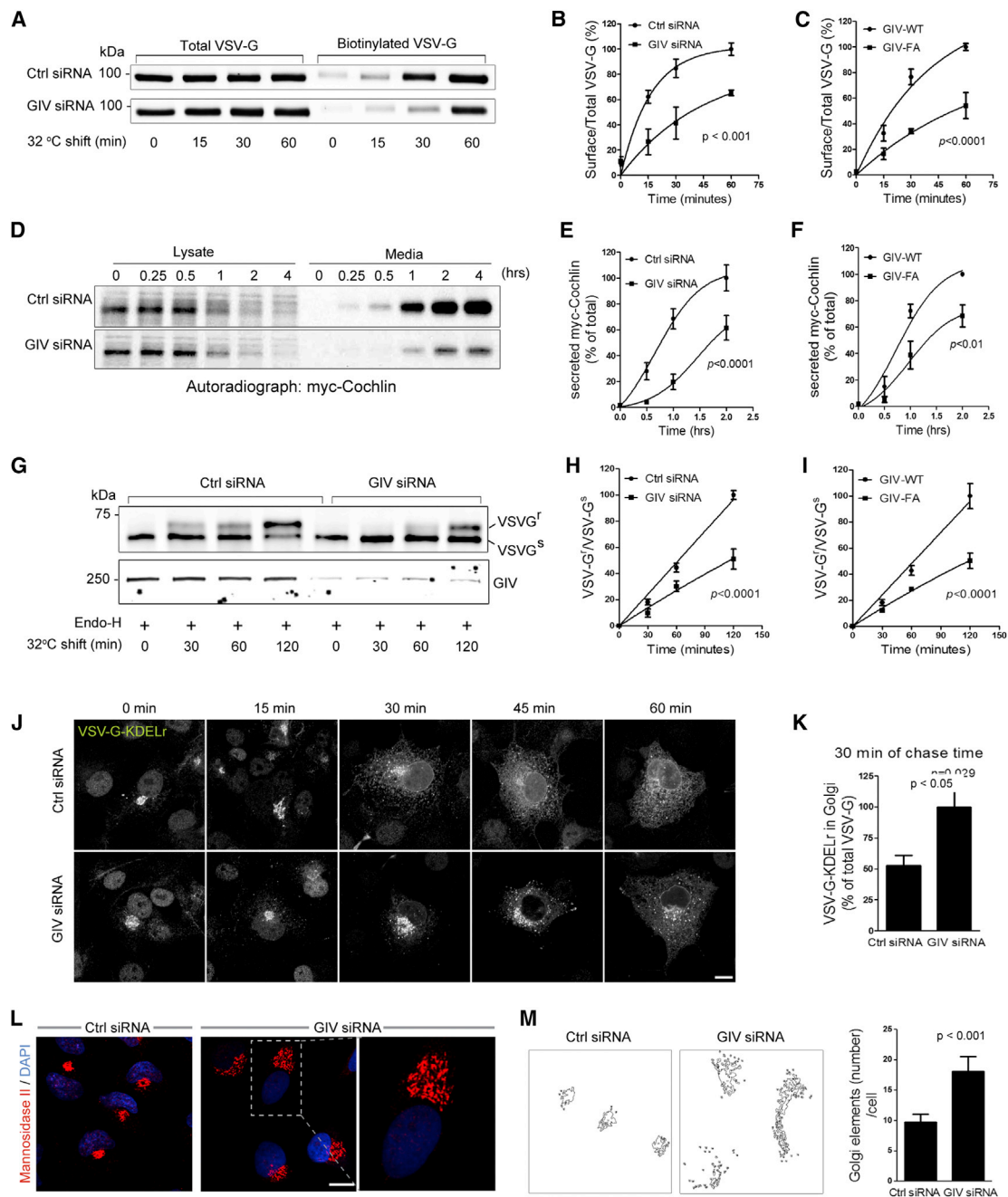
Figure 4. GIV and Its GEF Function Are Required for ER-Golgi Vesicle Transport and Integrity of the Golgi Structure

(A) Control (Ctrl siRNA) or GIV-depleted (GIV siRNA) COS7 cells were transfected with VSVG-tsO45-GFP and incubated at 40°C overnight before shifting to 32°C for the indicated times. Cell surface proteins were labeled with membrane-impermeable Sulfo-NHS-SS-Biotin as described in Supplemental Information. Surface biotinylated and total VSVG-GFP were analyzed by immunoblotting with anti-GFP.

(B) Graph displays the quantification of VSVG trafficking in control or GIV-depleted cells expressed as surface biotinylated to total VSVG-GFP, as determined by band densitometry. Data were normalized to control and expressed as % changes. (n = 3; error bars = SEM).

(C) Graph displays the quantification of VSVG trafficking (see Figure S4A) in cells expressing GIV-WT or GIV-FA calculated as in (B) (n = 4; error bars = SEM).

(D) Control (Ctrl siRNA) and GIV-depleted (GIV siRNA) HeLa cells transfected with myc-cochlin were pulsed with [^{35}S]Met-Cys (100 millicurie, 1/1,000 of a curie, a non-SI unit of radioactivity/ml) for 30 min, washed, and chased for the indicated times prior to lysis. Equal aliquots of media and cell lysates were immuno-precipitated with anti-myc mAb and analyzed for [^{35}S]-labeled-cochlin by autoradiography.

(E) Graph displays the quantification of results in (D), as determined by band densitometry and expressed as % myc-cochlin secreted in media/total myc-cochlin in lysates (n = 5).

(F) Graph displays the quantification of myc-cochlin secretion from HeLa cells stably expressing GIV-WT or GIV-FA (see Figure S4B) expressed as % myc-cochlin secreted in media/total myc-cochlin in lysates (n = 5).

(legend continued on next page)

biotinylation assays showed that compared to controls, in GIV-depleted cells the amount of VSVG that reached the PM at 30 and 60 min was reduced by ~40% and 30%, respectively (Figures 4A and 4B), indicating a delay in protein transport to the PM. Similarly, compared to cells expressing GIV-WT, VSVG trafficking to the PM was delayed in cells expressing GIV-FA (Figures 4C and S4A), indicating that GIV's GEF function is essential for GIV's role in VSVG trafficking. Release of myc-cochlin, a secretory protein, was also found to be delayed in GIV-depleted cells (Figures 4D and 4E) and in those expressing GIV-FA (Figures 4F and S4B). These results indicate that GIV is required for trafficking of two different cargo proteins in the secretory pathway, VSVG (a membrane protein) and myc-cochlin (a soluble protein), and that the GEF function is essential for GIV's role in regulation of such traffic.

Because COPI has been implicated in anterograde and retrograde traffic between the Golgi and the ER (Orci et al., 1997; Scheel et al., 1997), next we determined whether GIV depletion affects anterograde transport. We assessed the amount of VSVG that trafficked from ER to the Golgi, as determined by the degree of colocalization with the Golgi marker Man II at 32°C after 30 min. In controls, considerable VSVG accumulated in the Golgi within 5 min and was rapidly concentrated at the Golgi during subsequent time points. In GIV depleted cells (Figure S4C) or in cells expressing the GIV-insensitive Gαi3-WF mutant (Figure S4D), the amount of VSVG found in the Golgi was decreased at all time points (by ~35% at 30 min; Figure S4C). These findings indicate that both depletion of GIV and selective inhibition of GIV's ability to activate Gαi3 delays protein transport from the ER to the Golgi. Another strategy to assess the transport of VSVG-tsO45 from ER to Golgi is to detect acquisition of resistance to Endoglycosidase H (Endo-H) digestion of VSVG (Balch et al., 1986). When control cells were incubated at 40°C for 16 hr and then shifted to 32°C for 0–120 min, VSVG starts to acquire Endo-H-resistance by 30 min and the major pool of VGV-G acquires resistance by 120 min. In cells depleted of GIV, VSVG remains mostly sensitive to Endo-H at all points, indicative of a delay in VSVG trafficking from the ER to the early Golgi (Figures 4G and 4H). Furthermore, a majority of VSVG acquired Endo-H-resistance by 120 min in COS7 cells overexpressing GIV-WT, whereas VSVG remained sensitive to Endo-H in cells expressing inactive GIV-FA under the same conditions (Figures 4I and S4E), demonstrating that GIV's GEF function is essential for normal protein trafficking in the anterograde pathway.

To assess COPI-dependent retrograde trafficking, we analyzed the redistribution of a chimeric VSVG-tsO45-KDEL receptor (KDELr) from the Golgi to the ER by immunofluorescence (Cole et al., 1998). At 32°C this chimera accumulates in the cis-Golgi, and upon shifting the cells to 40°C, it redistributes to the ER via the retrograde pathway. In controls, the chimera had redistributed to the ER by 60 min at 40°C. However, in GIV-depleted cells, redistribution was substantially delayed, after 60 min the chimera was still present in ERGIC and the Golgi, as well as the ER (Figure 4J). The ratio of Golgi-associated to total VSVG-tsO45-KDELr fluorescence was ~2.2-fold higher in GIV-depleted cells than in controls at 30 min (Figure 4K). These results indicate that GIV is essential for both anterograde and retrograde COPI-mediated transport between the ER and Golgi.

GIV and Its GEF Function Maintain Golgi Ribbon Organization

Because Arf1 not only regulates vesicle transport, but also maintains Golgi structure (Dascher and Balch, 1994), we investigated if increased levels of active Arf1 in GIV-depleted cells also affect the structure of the Golgi. Staining for the cis- and medial-Golgi markers Man II (Figure 4L) and GM130 or the trans-Golgi marker GalT (Figure S4F) revealed that, as anticipated, the Golgi was compact and juxtanuclear in position in control cells. By contrast, in GIV-depleted cells, the Golgi stacks were unlinked and Golgi fluorescence was distributed across a larger number of structures (~80% increase; Figure 4M), although the total Golgi fluorescence was comparable to that in controls. Electron microscopy revealed that compared with control cells, the Golgi cisternae were reorganized into smaller, mini-stacks distributed over a broader area in GIV-depleted cells (Figure S4I). The Golgi was also dispersed in cells expressing either the GEF-deficient GIV-FA (Figure S4G) or GIV-insensitive Gαi3-WF (Figure S4H) mutants that cannot assemble a functional GIV-Gαi complex, indicating that GIV's ability to bind and activate the G protein is required for the integrity of Golgi stacks. These findings show that increased Arf1 activity in cells without a functional GIV-GEF is associated with aberrations in two fundamental processes regulated by Arf1; i.e., Golgi structure and function (vesicle trafficking).

(G) Control (Ctrl siRNA) or GIV-depleted (GIV siRNA) COS7 cells were infected with VSVG-tsO45 retrovirus for 1 hr at 32°C and shifted to 40°C for the next 16 hr. Cells were then shifted to 32°C for the indicated period of time prior to lysis. Equal aliquots of lysates were incubated with Endo-H (+) and subsequently analyzed for Endo-H-resistance (upward shift, upper panel) and GIV depletion (lower panel) by immunoblotting using anti-VSVG and anti-GIV, respectively.
(H) Graph displays the quantification of the data presented in (G), expressed as the ratio between Endo-H-resistant (VSVG^r; upper band) versus Endo-H-sensitive VGVG (VSVG^s; lower band) at various time points (n = 4).
(I) Graph displays the ratio between Endo-H-resistant versus sensitive VGVG in cells expressing GIV-WT or GIV-FA (n = 3) (see Figure S4E).
(J) Control (Ctrl siRNA) or GIV-depleted (GIV siRNA) COS7 cells transfected with chimeric tsO45-VSVG-KDELr-Myc were first incubated at 32°C and then shifted to 40°C (to allow transport of the chimeric receptor to the ER) for the indicated times, fixed, and stained for myc (white pixels). The scale bar represents 10 μm.
(K) Bar graph displays the % of the total tsO45-VSVG-KDELr-Myc within the Golgi region, quantified from confocal images of cells at 30 min (see Supplemental Information for details) (n = 3; five cells/experiment).
(L) Control (Ctrl siRNA) or GIV-depleted (GIV siRNA) COS7 cells were fixed and stained for Man II (red) and nuclei (DAPI; blue) and analyzed by confocal microscopy. Representative images of control or GIV-depleted cells are shown with a magnified view of the boxed area enlarged to the right. The scale bar represents 10 μm.
(M) Quantitative analysis of the Golgi phenotype in control and GIV-depleted cells by Image J (NIH) are shown (left panels). A fixed threshold was applied to all images, and objects were measured using the Analyze Particles function. Bar graphs (right) display the average number of Golgi elements per cell (n = 3; >14 cells/experiment).
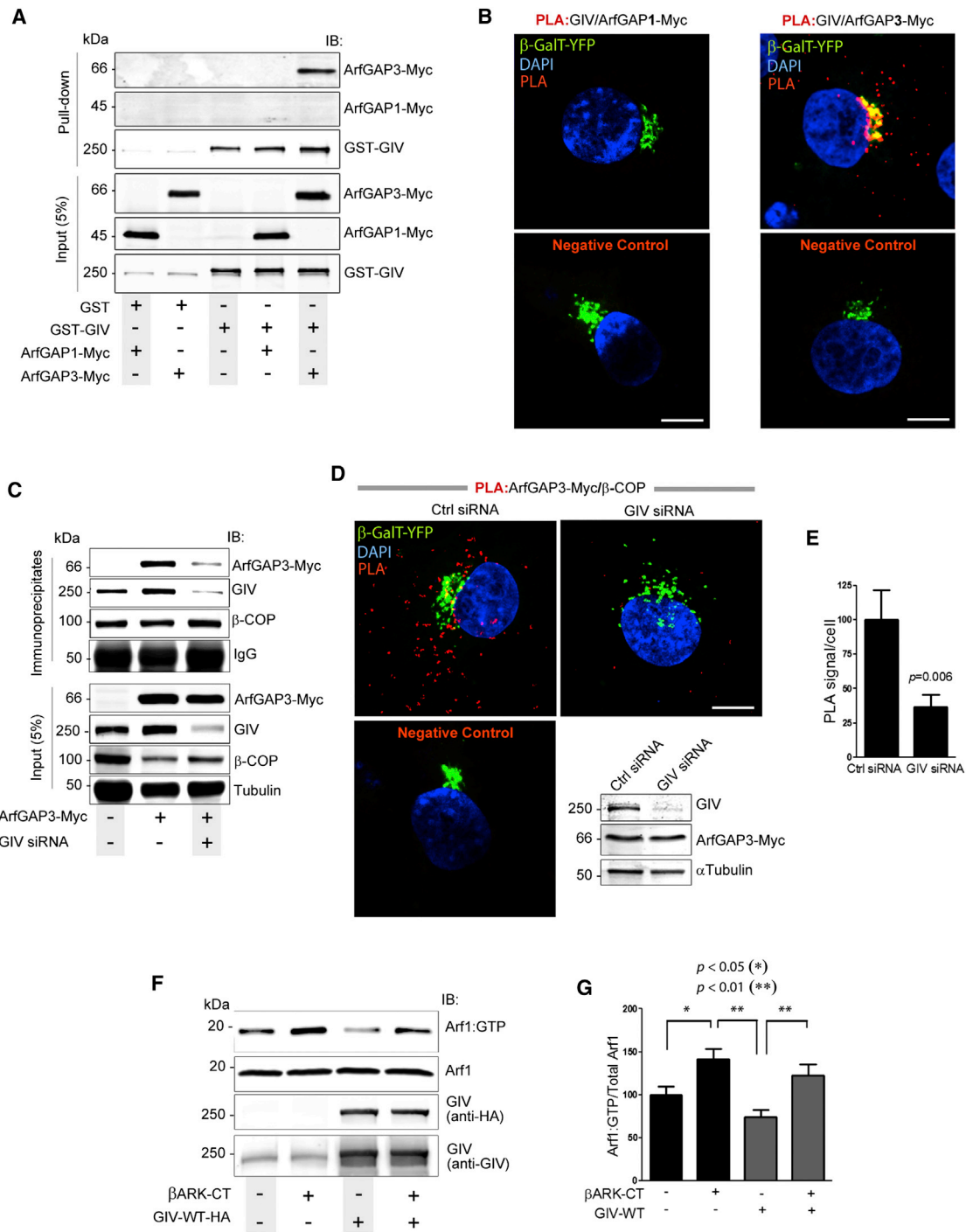
Figure 5. GIV Terminates Arf1 by Targeting ArfGAP3 to COPI Vesicles and Releasing Free Gβγ Dimers

(A) Lysates of COS7 cells coexpressing pCEFL-GST-GIV or GST alone (pCEFL-GST) and either ArfGAP1-myc (lanes 1 and 4) or ArfGAP3-myc (lanes 2 and 5) were incubated with glutathione-sepharose beads and bound proteins were analyzed by immmunoblotting.

(B) COS7 cells cotransfected with β-GalT-YFP (Golgi marker) and either ArfGAP1-Myc or ArfGAP3-Myc were analyzed for interaction between GIV and ArfGAPs by in situ PLA using rabbit anti-GIV and mouse-anti-myc antibodies. Similar distribution and expression of ArfGAPs 1 and 3 were verified by immunofluorescence (see Figure S5C). Incubation with primary antibodies was excluded for negative controls. Red dots = sites of interaction. The scale bar represents 10 μm.

(C) Immunoprecipitation was carried out on lysates from control (-) or GIV-depleted (GIV siRNA +) cells expressing ArfGAP3-myc using the CM1A10 (anti-coatomer) antibody. Inputs and immunoprecipitates were analyzed by immunoblotting. Band densitometry confirmed a ~60% reduction in ArfGAP3 in immune complexes from GIV-depleted cells.

(legend continued on next page)

GIV Regulates Arf1 via Its Ability to Bind ArfGAPs 2/3 and by Releasing Gβγ

Next, we explored how GIV suppresses Arf1 activity and explored GIV's interactions with the regulatory network of ArfGAP proteins (Weimer et al., 2008) that maintain finiteness of Arf1 signaling at the Golgi and on COPI vesicles. There are three Golgi-associated ArfGAPs which function in the COPI system, but at two distinct steps in vesicular transport. ArfGAP1 is assumed to drive the cycle of activation and inactivation of Arf1, and ArfGAP2 and ArfGAP3 are believed to regulate uncoating (Beck et al., 2009; Shiba and Randazzo, 2012). We reasoned that GIV might regulate Arf1·GTP at the step of uncoating through ArfGAPs 2/3. We found that GIV specifically bound ArfGAP2/3, but not ArfGAP1 in pull-down assays (Figures 5A and S5A). Such specificity was also confirmed by in situ PLA studies, numerous sites of GIV-ArfGAP interactions were seen in cells expressing ArfGAP3-Myc, but no such interactions were observed in cells expressing ArfGAP1-Myc (Figure 5B).

Next, we investigated whether GIV affects the association of ArfGAP3 with COPI-coated membranes. Immunoprecipitation was carried out with anti-CM1A10 IgG from lysates of control and GIV-depleted cells expressing ArfGAP3-Myc. Interaction of ArfGAP3-Myc with coatomer was greatly reduced in GIV-depleted cells (Figure 5C) despite the abundance of β-COP on membranes (Figures 2D and 2E). In situ PLA studies confirmed that depletion of GIV was associated with a ~60% reduction in the number of sites of interaction between ArfGAP3-Myc and coatomer (Figures 5D, 5E, and S5B). A similar reduction was also observed in Golgi localization of ArfGAP3, but not ArfGAP1 in GIV-depleted cells by immunofluorescence (Figure S5C). These results demonstrate that GIV is required for the association of ArfGAP3 with COPI vesicles and Golgi membranes, and that failure of such association in GIV-depleted cells may contribute, in part, to the elevated levels of Arf1·GTP and accumulation of COPI vesicles we observe in these cells. Because GIV also binds ArfGAP2 (Figure S5A), which shares a high degree of sequence identity with ArfGAP3 (Frigerio et al., 2007) and complements the functions of ArfGAP3 (Weimer et al., 2008), it is likely that GIV affects the localization and activation of both ArfGAPs 2 and 3.

Because GIV's ability to affect Arf1 activity is also dependent on its ability to activate Gαi, next we asked how GIV may link trimeric G protein signaling to the regulation of Arf activity. Prior work has implicated "free" Gβγ subunits of G proteins as inhibitors of Arf1 activity on Golgi membranes (Donaldson et al., 1991). We asked if inhibition of Arf1·GTP by GIV-GEF is a consequence of release of Gβγ upon Gi activation. To investigate this, we used a well-characterized peptide corresponding to the C terminus of the β-adrenergic receptor kinase (βARK-CT) that sequesters Gβγ. Consistent with the role of Gβγ in downregulation of Arf1 activity, sequestration of Gβγ in COS7 cells transfected with βARK-CT was associated with an elevation of Arf1·GTP levels (Figures 5F and 5G). Suppression of Arf1 activity in cells overexpressing GIV-WT was reversed when βARK-CT was coexpressed with GIV-WT. Noteworthy, the levels of Arf1 activity in cells coexpressing βARK-CT and GIV-WT were intermediate between the high levels of activity in cells expressing βARK-CT alone and the low levels of activity in cells expressing GIV-WT alone, indicating that βARK-CT and GIV-WT antagonistically modulate Arf1 activity, presumably via their ability to sequester or release, respectively, free Gβγ subunits. Furthermore, sequestration of free Gβγ subunits by βARK-CT delayed VSVG trafficking to the PM (Figure S5D) and dispersed the Golgi ribbon structure (Figure S5E). Noteworthy, these phenotypes resemble that of cells in which GIV-dependent activation of Gi and subsequent release of free Gβγ is impaired (by expressing either a GEF-deficient GIV-FA mutant or a GIV-insensitive Gαi3-WF mutant; Figures 4 and S4). These data demonstrate that the availability of free Gβγ is critical for termination of Arf1 activity and for the functional and structural integrity of the Golgi; either sequestration (by βARK-CT) or impaired release of Gβγ (absence of a functional GIV-GEF) leads to enhanced Arf1 activity. Taken together, our findings indicate that GIV suppresses the levels of active Arf1 and regulates ER-Golgi transport and Golgi structure in part via activation of Gi and release of free Gβγ.

GIV Binds Active Arf1

Next, we explored what event might trigger GIV-dependent termination of Arf1 activity and vesicle uncoating. We hypothesized that targeting of GIV to membranes with active Arf1 could be one such event that sets off negative feedback loops allowing GIV to subsequently terminate Arf1 signaling. Because active Arf1 regulates membrane association of several proteins involved in vesicle trafficking (Donaldson and Jackson, 2011), we asked whether Arf1 also affects the membrane association of GIV. We found that membrane-associated GIV was increased by ~30% in cells expressing the constitutively active Arf1 mutant, Arf1[Q71L], compared to those expressing the dominant-negative mutant, Arf1[T31N] (Figures 6A and 6B). By immunofluorescence, we confirmed Golgi membranes as the major site for Arf1-dependent recruitment of GIV, where both proteins colocalized (Figures 6C and S6A). When we carried out immunoprecipitation assays from lysates of human embryonic kidney (HEK)293 cells coexpressing Arf1-HA and GIV-FLAG, we found that Arf1 coimmunoprecipitates with GIV (Figure 6D). When recombinant myristoylated Arf1 was loaded with guanosine diphosphate (GDP) (inactive conformation) or Guanosine 5'-[β,gamma-imido]triphosphate (5'-Guanylyl-imido-diphosphate trisodium salt hydrate [GMP-PNP], to mimick active conformation) and incubated with purified GST-GIV or GST alone, Arf1 loaded with GMP-PNP, but not GDP specifically bound to GIV (Figure 6E), indicating that the Arf1-GIV interaction is direct and that GIV preferentially binds active Arf1. Together, these data show that GIV binds active Arf1 and that activation

(D) Control (Ctrl siRNA) or GIV-depleted (GIV siRNA) COS7 cells cotransfected with β-GalT-YFP (Golgi marker) and ArfGAP3-Myc were analyzed for interaction between β-COP and ArfGAP3-Myc by in situ PLA. Incubation with primary antibodies was excluded for negative controls. Red dot = sites of interaction. The scale bar represents 10 μm. Depletion of GIV and equal transfection of ArfGAP3-Myc were confirmed by IB (inset).

(E) Bar graphs display the quantification of interactions (n = 3; >20 cells/experiment) in (D).

(F) Lysates of COS7 cells expressing GIV-WT, βARK-CT, and control vector (-) were analyzed for Arf1·GTP using GST pull-down assays as in Figure 3B.

(G) Bar graphs display the quantification of the data in (F), expressed as the ratio of Arf1·GTP to total Arf1. Results were presented as mean ± SEM (n = 5).
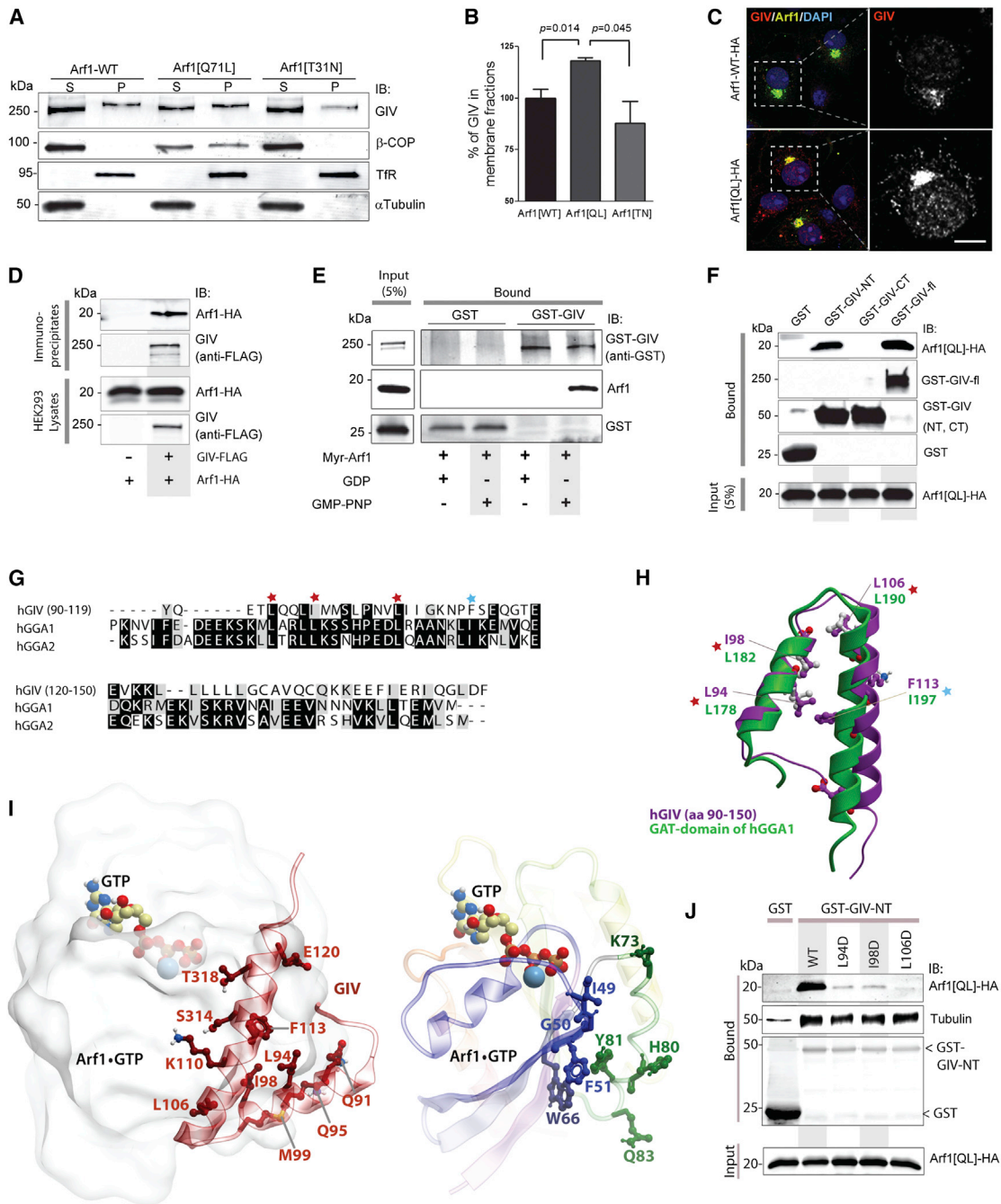
Figure 6. Active Arf1 Binds GIV and Triggers Its Membrane Association

(A) Membrane-cytosol fractionations were carried out on COS7 cells expressing HA-tagged WT, constitutively active (Q71L), or dominant-negative (T31N) Arf1, and fractions were analyzed for GIV and β-COP as in Figure 2D.

(B) Bar graph displays the % GIV in membrane (P) fractions derived from (P)/(S + P) × 100. Results are expressed as mean ± SEM.

(C) COS7 cells transfected with HA-tagged WT Arf1 or Arf1[Q71L] mutant were fixed and stained for Arf1 (HA; green), GIV (red), and nuclei (DAPI; blue). Panels on the left show an overlay of all three stains (see Figure S6A for individual stains), whereas panels on the right display the red pixels in grayscale, which represent GIV.

(D) Immunoprecipitation was carried out from lysates of HEK293T cells expressing Arf1-HA alone or Arf1-HA and GIV-FLAG using anti-FLAG mAb, and bound immune complexes were analyzed for Arf (HA) and GIV by immunoblotting.

(E) Purified myristoylated Arf1 preloaded with GDP or GMP-PNP was incubated with GST or GST-GIV (expressed and purified from HEK293T cells) immobilized on glutathione beads. Bound proteins were analyzed for Arf1 and GIV by immunoblotting.

(F) Lysates of HEK293T cells coexpressing HA-tagged Arf1[Q71L] and GST or GST-tagged GIV constructs (GIV-NT, 1–220 aa; GIV-CT, 1,660–1,870 aa; GIV-fl, 1–1,870 aa) were incubated with glutathione beads. Bound proteins were analyzed for Arf1 and GST proteins by immunoblotting.

(legend continued on next page)

of Arf1 enhances recruitment of GIV on Golgi membranes and may initiate/trigger the interaction between GIV and COPI-coated membranes we observe (see Figure 2).

To determine how GIV binds Arf1, we carried out protein interaction assays with different GST-tagged domains of GIV and found that the N-terminal ∼200 amino acids (aa) of GIV, the Hook domain, is sufficient to interact with constitutively active Arf1[Q71L] (Figure 6F). A sequence alignment between GIV's Hook domain and the GAT domain of the GGA family of proteins, which binds active Arf1, revealed a striking similarity in sequence (Figure 6G). Three critical leucines that have been previously implicated in mediating the interaction between Arf1·GTP and a Hook-like patch on the GGA-GAT domain (Collins et al., 2003; Shiba et al., 2003) are evolutionarily conserved in GIV (Figures 6G and S6B). A homology model of this region generated using the previously solved crystal structure of the GGA-GAT domain (Shiba et al., 2003) revealed a helix-loop-helix conformation much like that assumed by the Hook-like patch within the GGA-GAT domain (Figure 6H). Using the available structure of the Arf1·GTP:GGA1-GAT complex as a template (Protein Data Bank [PDB] 1J2J), we modeled the Arf1·GTP:GIV interface and found that key residues that were conserved between GGA and GIV are required to form the Arf1·GIV interface (Figure 6I). Using pull-down assays with active Arf1[Q71L] mutant and the GST-tagged Hook domain of GIV, we confirmed that mutation of the key residues disrupted Arf1·GIV interaction as predicted (Figure 6J), thereby validating the homology model (Figure 6I). These results demonstrate that GIV preferentially binds active Arf1 in a manner identical to GGA proteins and, thereby, serves as an effector of active Arf1 at the Golgi.

Conclusions

These studies identify GIV as a bona fide activator of heterotrimeric G proteins at the Golgi and as a platform for crosstalk between trimeric G proteins and the monomeric GTPase Arf1. Such crosstalk via GIV regulates both vesicle trafficking and the organization of Golgi stacks. Our results provide mechanistic insights into how GIV orchestrates a two-pronged mechanism to suppress Arf1 signaling when COPI vesicles carrying cargo proteins from the ER/ERGIC dock on the Golgi membranes (see Figure 7), first, activation of Gαi by GIV at the Golgi complex releases free Gβγ, which in turn inhibits Arf1 signaling. Second, GIV interacts with both β-COP and ArfGAP2/3 and facilitates the recruitment

of the coat-dependent GAP protein onto the Golgi and COPI vesicles. Once recruited, the catalytic activity of ArfGAP2/3 is enhanced, presumably at/near the target Golgi membranes, and consequently Arf1 signaling is efficiently terminated and COPI vesicles uncoat prior to fusion.

The first event; i.e., activation of Gi by GIV and release of Gβγ (GIV→Gβγ pathway) on Golgi membranes, is a hierarchically dominant step because without a functional GEF motif in GIV, ArfGAP3 localized to Golgi/COPI vesicles normally (Figure S7A), but Arf1 activity remained elevated, vesicle uncoating was impaired, trafficking was delayed, and Golgi ribbons were dispersed. Activation of Gi and release of free Gβγ dimers is also a central mechanism by which GIV terminates Arf1 at/near acceptor (i.e., Golgi) membranes and is consistent with prior work demonstrating the inhibitory role of Gβγ in Arf signaling (Cohen and Donaldson, 2010; Colombo et al., 1995). Although hierarchically dominant, the GIV→Gβγ pathway is dependent on the GIV→ArfGAP2/3 pathway, because the ability of GIV-GEF to downregulate Arf1 activity is abolished in cells without ArfGAP3 (Figure S7B). These findings suggest that the GIV→Gβγ and the GIV→ArfGAP2/3 pathways work in-tandem and/or synergize with each other to terminate Arf1 signaling and complete uncoating of vesicles tethered to Golgi membranes. Such synergy on Golgi membranes may impart directionality to anterograde ER-Golgi transport.

As to what upstream event sets off the GIV→Gβγ and the GIV→ArfGAP2/3 pathways, which culminate in termination of Arf1 signaling, we show that recruitment of GIV to membranes by direct binding to active Arf1 could be the likely trigger. Based on its ability to bind Arf1·GTP and PI(4)P (Figure 7; see Enomoto et al., 2005), GIV joins the handful of PI(4)P effectors whose recruitment to the Golgi also requires activated Arf1 (Mayinger, 2011). Such dual recognition is believed to function in a "coincidence-detection" mechanism that provides additional specificity to achieve restricted localizations on membrane microdomains (Carlton and Cullen, 2005). We propose that GIV is recruited specifically to the membrane microdomains that have active Arf1 to impose finiteness to Arf1 signaling, trigger uncoating of COPI vesicles, and thereby affect the anterograde trafficking of secreted and membrane proteins along the exocytic pathway, all via a network of hierarchical functional interactions, mediated by distinct modules (Figure 7, upper panel). The abnormalities we observe in retrograde trafficking could either

(G) Sequence alignment of GIV with GGA proteins reveals a putative GGA-GAT like region within the Hook domain of GIV. The sequence corresponding to the N-terminal Hook domain of human GIV (BAE44387, 90–150 aa) was aligned with the sequence of human GGA1/2 proteins using CLUSTAL W. Conserved residues are shaded in black; similar residues in gray. This alignment reveals that the key aa that are essential for Arf1·GGA-GAT interaction are conserved in GIV. The residues marked with red star were mutated in this work to confirm that they are essential for the Arf1:GIV interaction.

(H) 3D model of 90–150 aa within GIV's Hook domain (purple) superimposed on the solved structure of the Hook-like patch on GAT domains of human GGA1 protein (green), generated based on the alignment in (G). Key residues in GGA that are important for coupling to Arf1·GTP and the corresponding residues in GIV are labeled.

(I) 3D model of a complex between Arf1·GTP (colored by blue/green/yellow/red rainbow from N to C terminus) and the N-terminal helix-loop-helix motif of GIV (dark red). GTP and an Mg ion are shown as colored sticks and a blue sphere, respectively. Left panel shows the overall complex with the most important interface residues in GIV. The right panel shows the most important interface residues in Arf1. The binding occurs at the loosely helical Arf1 loop "switch 1" (blue, containing isoleucine at 49, glycine at 50) and also involves β2/3-strands (blue, containing F51 and W66) and the second alpha helix (green, containing H80 and Y81). Residues L94, I98, I106, and F113 form the core of the hydrophobic patch on GIV's helix-loop-helix motif that interacts with residues F51, W66, and Y81 in Arf1. Multiple polar contacts surrounding this patch may additionally strengthen the Arf1·GTP:GIV interaction and provide specificity.

(J) Lysates of HEK293T cells coexpressing HA-tagged Arf1[Q71L] and WT or mutant GST-tagged GIV-NT 1–220 aa constructs (L94D, I98D, and L106D) were incubated with glutathione beads. Bound proteins were analyzed for Arf1 and GST proteins by immunoblotting. As expected for a Hook domain, WT, and all mutant GIV-NT proteins bound tubulin.
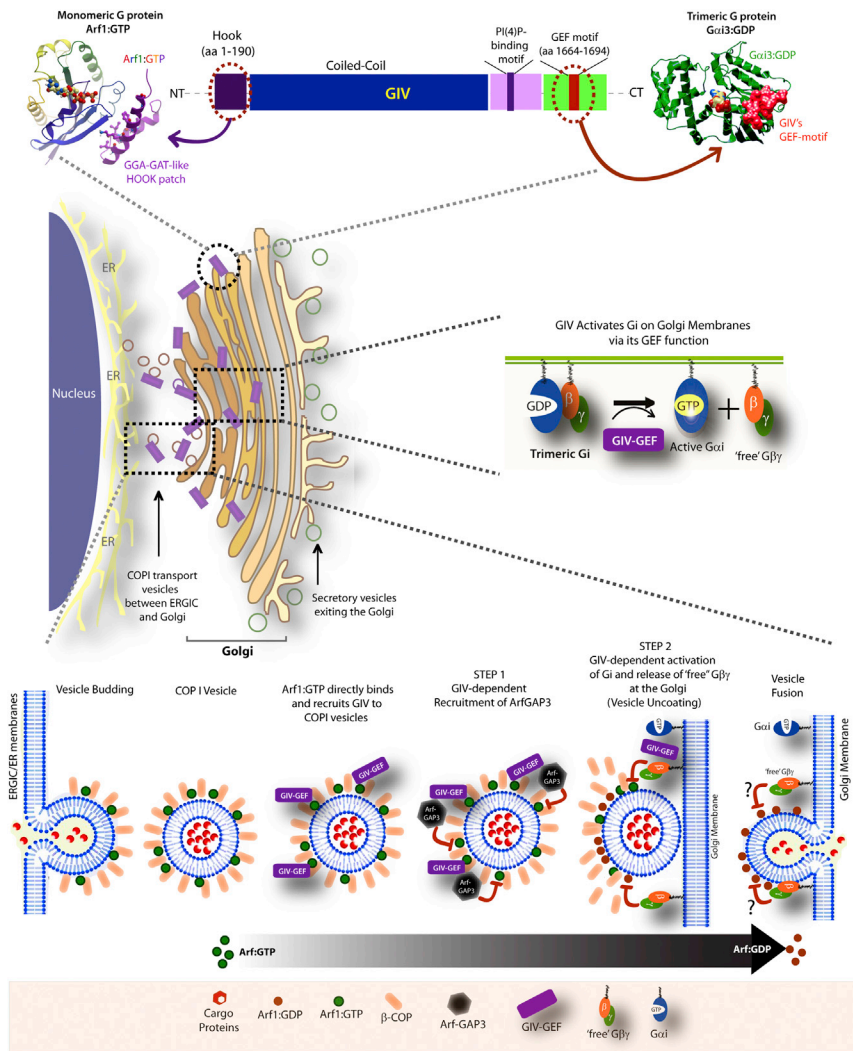
Figure 7. Summary and Working Model

(Upper), schematic of the multi-modular GIV protein is shown. A patch of residues within the N-terminal Hook-domain of GIV (purple) resembles the Hook-like patch within the GAT domain of GGA1/2/3 proteins and directly binds GTP-bound Arf1. The coiled-coil domain (blue) assists in homooligomerization, whereas the PI(4)P-binding domain mediates binding to phosphoinositides at the Golgi and the PM (Enomoto et al., 2005). The C-terminally located GEF motif (red) of GIV binds and activates Gαi, and releases free Gβγ. Homology models shown for Arf1:GIV-Hook (left) is validated in current work (Figure 6) and that for Gαi3 (green):GIV-GEF (red) was validated previously (right; see Garcia-Marcos et al., 2009). (Middle), schematic of perinuclear Golgi compartment is shown. GIV is a GEF for Gαi that activates trimeric G proteins on Golgi membranes and releases free Gβγ dimers. (Lower), schematic of hierarchical steps that enable GIV to terminate Arf1 signaling and trigger COPI coatomer dissociation during anterograde trafficking. From left to right, membrane-associated Arf1·GTP recruits COPI coatomer (represented here as β-COP) onto membranes and promotes vesicle budding from the ER/ERGIC compartment. GIV is recruited to COPI vesicles, presumably as an effector of active Arf1, and further stabilized by its ability to interact with the coat protein, β-COP. Once on vesicles, GIV binds and recruits ArfGAP3, which is required for terminating Arf1 activity and initiating the process of uncoating (STEP 1). Termination of Arf1 activity is further perpetuated by a second step (STEP 2), which involves activation of Gi and release of free Gβγ by GIV on Golgi membranes. This second step presumably takes place only when COPI vesicles dock on Golgi membranes (i.e., acceptor membrane) and serves to terminate any remaining active Arf1 on those vesicles via pathway(s) that remain unclear (""?) and ensure completion of the uncoating process just prior to vesicle fusion.

be a direct or an indirect consequence of delayed anterograde trafficking, as the two processes are interdependent (Reilly et al., 2001). We showed that modulation of Arf1 signaling by GIV also maintains Golgi structure, and in the absence of GIV, Golgi stacks are reorganized into unlinked mini-stacks scattered over a larger area. Thus, our findings reveal the fundamental molecular mechanisms behind the previously observed roles of G proteins at the Golgi; e.g., membrane trafficking (Simpson et al., 2012), vesicle fusion, (Helms et al., 1998), and in the maintenance of Golgi structure (Saini et al., 2010). Because G proteins and the other essential components (Arf1, ArfGAP3, and GIV) are also present on other membranes, it is possible that the fundamental mechanisms we define here also facilitate vesicular trafficking from the *trans*-Golgi network (TGN) to the PM and/or endolysosomal system, as shown in the case of ArfGAP3 (Shiba et al., 2013).

With regard to ArfGAPs, our finding that GIV selectively binds and localizes ArfGAP2/3 (but not ArfGAP1) to COPI vesicles to trigger vesicle uncoating are consistent with the fact that ArfGAP1 triggers vesicle formation (Cole et al., 1998; Shiba and Randazzo, 2012), whereas ArfGAPs 2/3 trigger uncoating

(Shiba and Randazzo, 2012). Although ArfGAP3 is reported to be a coat protein-dependent ArfGAP (Schindler et al., 2009; Weimer et al., 2008), i.e., both its association with COPI vesicles and its GAP activity are triggered by coat proteins (Kliouchnikov et al., 2009), β-COP, the major coat-protein on COPI vesicles does not fulfil such a role (Weimer et al., 2008). It is thus possible that GIV serves as the long-sought coatomer-associated cofactor for ArfGAP3. We conclude that GIV's ability to bind and localize ArfGAP3 to COPI vesicles is one arm of the two-pronged mechanism that enables GIV to terminate Arf1 signaling and trigger vesicle uncoating; whether the other arm, i.e., GIV→Gβγ pathway, directly enhances the catalytic activity of ArfGAP3 on the membranes remains to be determined.

Finally, we show that the multi-modular make-up of GIV enables it to serve as a platform for crosstalk between heterotrimeric G proteins and monomeric Arf G proteins (Figure 7, top panel). The paradigm of dual regulation of monomeric and trimeric G proteins by a single protein has been previously demonstrated in only a handful of proteins and is exemplified by p115RhoGEF (Kozasa et al., 1998). However, GIV serves as the only molecule to date that links trimeric G protein signaling

on membranes to inactivation of Arf1, and thereby, acts as an intermediary in the regulation of Arf proteins by G proteins. Because full-length GIV is evolutionarily young (i.e., found only in higher eukaryotes like birds and mammals) (Ghosh et al., 2011), coupling of trimeric G protein signaling with monomeric Arf G proteins by GIV likely represents an evolutionary improvement to meet the demands of increasingly complex trafficking itineraries in higher eukaryotes. Finally, that GIV localizes also at the PM and modulates pro-migratory and mitogenic growth factor signals via activation of Gαi raises the possibility that the previously observed crosstalk between growth factor signals initiated at the PM and functions of the Golgi (Blagoveshchenskaya et al., 2008; Weller et al., 2010) may be orchestrated in part via the GIV platform. Such crosstalk may coordinately trigger secretion in response to pro-migratory signals when the GIV-GEF is activated and/or coordinate the dispersal of Golgi in response to mitogenic signals when the GIV-GEF is disabled. Thus, the crosstalk GIV sets up between trimeric G proteins and monomeric Arf G proteins at two locations within the cell may represent another evolutionary advantage that allows for regulation of Golgi functions by external environmental cues.

In conclusion, we have defined GIV as a bona fide activator of the trimeric G protein Gαi at the Golgi and an effector of active Arf1, and we have demonstrated that activation of Gi by GIV serves the fundamental role of ensuring finiteness of Arf1 signaling at the Golgi. Consequently, GIV regulates both structure and function of the Golgi, two closely intertwined processes regulated by Arf1. Thus, this work elucidates some of the well-known, but poorly understood functions of G proteins on intracellular membranes and impacts our understanding of trimeric G protein signaling in the secretory pathway.

EXPERIMENTAL PROCEDURES

Detailed methods are stated in Supplemental Information.

Purification of GST-GAT protein and assessment of Arf1 activation were described previously (Cohen and Donaldson, 2010). Immunofluorescence and confocal microscopy was performed as described previously (Ghosh et al., 2010).

PLA

These were done using a Duolink Kit (Sigma) according to the manufacturer's instructions.

FRET Studies

Previously validated internally tagged Gαi$_1$-YFP and CFP-Gβ$_1$γ$_2$ FRET probe pairs were used (Bünemann et al., 2003; Gibson and Gilman, 2006). FRET efficiency was calculated on a pixel by pixel basis from the normalized ratiometric images obtained individually in donor, FRET, and acceptor channels. For FRET quantification, regions of interest (ROI) were drawn in the juxtanuclear area presumably in the Golgi region to compute energy transfer. Individual cells with fluorescence intensity in the mesoscopic regime detected in the donor and acceptor channels were selected for FRET analysis to avoid inhomogeneities between samples.

GFP-tsO45-VSVG Transport Assays

To monitor anterograde (ER to Golgi) trafficking, COS7 cells were treated overnight with control or GIV siRNA and transiently transfected with GFP-tsO45-VSVG plasmid (Presley et al., 1997). Transfected cells were incubated for 14–16 hr at the restrictive temperature (40°C) to accumulate VSVG protein in

the ER, shifted to 32°C for 0–60 min to release VSVG protein and then fixed and processed for immunofluorescence. The rate of VSVG trafficking from the ER to the Golgi was determined by calculating the ratio of Golgi-associated VSVG, determined by colocalization with Man II, and total VSVG fluorescence, using Image J (NIH) software.

Construction of a 3D Model of Arf1 Interaction with the N-Terminal Helix-Loop-Helix Motif of GIV

The homology model of the Arf1:GIV complex was constructed using the ICM comparative (homology) modeling procedure using the structure of constitutively active Arf1 in complex with the N-terminal GAT domain of human GGA1 (PDB 1J2J) as a template and guided by the GIV/GGA1 sequence alignment in Figure 6G. The initial model was generated by assigning the backbone coordinates of both target molecules (Arf1 and GIV) to their counterparts in the template. This model was further refined using extensive sampling of residue side chains in internal coordinates and then additionally relaxed by full-atom local minimization in the presence of distance restraints, while maintaining the conserved hydrogen bonds, protein secondary structure, and topology.

SUPPLEMENTAL INFORMATION

Supplemental Information includes Supplemental Experimental Procedures and seven figures and can be found with this article online at http://dx.doi.org/10.1016/j.devcel.2015.02.009.

AUTHOR CONTRIBUTIONS

ACKNOWLEDGMENTS

REFERENCES

Balch, W.E., Elliott, M.M., and Keller, D.S. (1986). ATP-coupled transport of vesicular stomatitis virus G protein between the endoplasmic reticulum and the Golgi. J. Biol. Chem. 261, 14681–14689.

Barr, F.A., Leyte, A., and Huttner, W.B. (1992). Trimeric G proteins and vesicle formation. Trends Cell Biol. 2, 91–94.

Beck, R., Rawet, M., Wieland, F.T., and Cassel, D. (2009). The COPI system: molecular mechanisms and function. FEBS Lett. 583, 2701–2709.

Blagoveshchenskaya, A., Cheong, F.Y., Rohde, H.M., Glover, G., Knödler, A., Nicolson, T., Boehmelt, G., and Mayinger, P. (2008). Integration of Golgi trafficking and growth factor signaling by the lipid phosphatase SAC1. J. Cell Biol. 180, 803–812.

Bünemann, M., Frank, M., and Lohse, M.J. (2003). Gi protein activation in intact cells involves subunit rearrangement rather than dissociation. Proc. Natl. Acad. Sci. USA 100, 16077–16082.

Cancino, J., and Luini, A. (2013). Signaling circuits on the Golgi complex. Traffic 14, 121–134.

Carlton, J.G., and Cullen, P.J. (2005). Coincidence detection in phosphoinositide signaling. Trends Cell Biol. 15, 540–547.

Cohen, L.A., and Donaldson, J.G. (2010). Analysis of Arf GTP-binding protein function in cells. Curr. Protoc. Cell Biol. Chapter 3. Unit 14.12.1–17.

Cole, N.B., Ellenberg, J., Song, J., DiEuliis, D., and Lippincott-Schwartz, J. (1998). Retrograde transport of Golgi-localized proteins to the ER. J. Cell Biol. 140, 1–15.

Collins, B.M., Watson, P.J., and Owen, D.J. (2003). The structure of the GGA1-GAT domain reveals the molecular basis for ARF binding and membrane association of GGAs. Dev. Cell 4, 321–332.

Colombo, M.I., Inglese, J., D'Souza-Schorey, C., Beron, W., and Stahl, P.D. (1995). Heterotrimeric G proteins interact with the small GTPase ARF. Possibilities for the regulation of vesicular traffic. J. Biol. Chem. 270, 24564–24571.

Dascher, C., and Balch, W.E. (1994). Dominant inhibitory mutants of ARF1 block endoplasmic reticulum to Golgi transport and trigger disassembly of the Golgi apparatus. J. Biol. Chem. 269, 1437–1448.

Donaldson, J.G., and Jackson, C.L. (2011). ARF family G proteins and their regulators: roles in membrane transport, development and disease. Nat. Rev. Mol. Cell Biol. 12, 362–375.

Donaldson, J.G., Kahn, R.A., Lippincott-Schwartz, J., and Klausner, R.D. (1991). Binding of ARF and beta-COP to Golgi membranes: possible regulation by a trimeric G protein. Science 254, 1197–1199.

Enomoto, A., Murakami, H., Asai, N., Morone, N., Watanabe, T., Kawai, K., Murakumo, Y., Usukura, J., Kaibuchi, K., and Takahashi, M. (2005). Akt/PKB regulates actin organization and cell motility via Girdin/APE. Dev. Cell 9, 389–402.

Frigerio, G., Grimsey, N., Dale, M., Majoul, I., and Duden, R. (2007). Two human ARFGAPs associated with COP-I-coated vesicles. Traffic 8, 1644–1655.

Gallione, C.J., and Rose, J.K. (1985). A single amino acid substitution in a hydrophobic domain causes temperature-sensitive cell-surface transport of a mutant viral glycoprotein. J. Virol. 54, 374–382.

Garcia-Marcos, M., Ghosh, P., and Farquhar, M.G. (2009). GIV is a nonreceptor GEF for G alpha i with a unique motif that regulates Akt signaling. Proc. Natl. Acad. Sci. USA 106, 3178–3183.

Garcia-Marcos, M., Ghosh, P., Ear, J., and Farquhar, M.G. (2010). A structural determinant that renders G alpha(i) sensitive to activation by GIV/girdin is required to promote cell migration. J. Biol. Chem. 285, 12765–12777.

Garcia-Marcos, M., Ghosh, P., and Farquhar, M.G. (2015). GIV/ Girdin transmits signals from multiple receptors by triggering trimeric G protein activation. J. Biol. Chem. 290, 6697–6704.

Ghosh, P., Beas, A.O., Bornheimer, S.J., Garcia-Marcos, M., Forry, E.P., Johannson, C., Ear, J., Jung, B.H., Cabrera, B., Carethers, J.M., and Farquhar, M.G. (2010). A Galphai-GIV molecular complex binds epidermal growth factor receptor and determines whether cells migrate or proliferate. Mol. Biol. Cell 21, 2338–2354.

Ghosh, P., Garcia-Marcos, M., and Farquhar, M.G. (2011). GIV/Girdin is a rheostat that fine-tunes growth factor signals during tumor progression. Cell Adhes. Migr. 5, 237–248.

Gibson, S.K., and Gilman, A.G. (2006). Gialpha and Gbeta subunits both define selectivity of G protein activation by alpha2-adrenergic receptors. Proc. Natl. Acad. Sci. USA 103, 212–217.

Gilman, A.G. (1987). G proteins: transducers of receptor-generated signals. Annu. Rev. Biochem. 56, 615–649.

Helms, J.B., Helms-Brons, D., Brügger, B., Gkantiragas, I., Eberle, H., Nickel, W., Nürnberg, B., Gerdes, H.H., and Wieland, F.T. (1998). A putative heterotrimeric G protein inhibits the fusion of COPI-coated vesicles. Segregation of heterotrimeric G proteins from COPI-coated vesicles. J. Biol. Chem. 273, 15203–15208.

Hewavitharana, T., and Wedegaertner, P.B. (2012). Non-canonical signaling and localizations of heterotrimeric G proteins. Cell. Signal. 24, 25–34.

Kliouchnikov, L., Bigay, J., Mesmin, B., Parnis, A., Rawet, M., Goldfeder, N., Antonny, B., and Cassel, D. (2009). Discrete determinants in ArfGAP2/3 conferring Golgi localization and regulation by the COPI coat. Mol. Biol. Cell 20, 859–869.

Kozasa, T., Jiang, X., Hart, M.J., Sternweis, P.M., Singer, W.D., Gilman, A.G., Bollag, G., and Sternweis, P.C. (1998). p115 RhoGEF, a GTPase activating protein for Galpha12 and Galpha13. Science 280, 2109–2111.

Lane, J.R., Henderson, D., Powney, B., Wise, A., Rees, S., Daniels, D., Plumpton, C., Kinghorn, I., and Milligan, G. (2008). Antibodies that identify only the active conformation of G(i) family G protein alpha subunits. FASEB J. 22, 1924–1932.

Le-Niculescu, H., Niesman, I., Fischer, T., DeVries, L., and Farquhar, M.G. (2005). Identification and characterization of GIV, a novel Galpha i/s-interacting protein found on COPI, endoplasmic reticulum-Golgi transport vesicles. J. Biol. Chem. 280, 22012–22020.

Mayinger, P. (2011). Signaling at the Golgi. Cold Spring Harb. Perspect. Biol. 3, 3.

Oprins, A., Duden, R., Kreis, T.E., Geuze, H.J., and Slot, J.W. (1993). Beta-COP localizes mainly to the cis-Golgi side in exocrine pancreas. J. Cell Biol. 121, 49–59.

Orci, L., Stamnes, M., Ravazzola, M., Amherdt, M., Perrelet, A., Söllner, T.H., and Rothman, J.E. (1997). Bidirectional transport by distinct populations of COPI-coated vesicles. Cell 90, 335–349.

Palmer, D.J., Helms, J.B., Beckers, C.J., Orci, L., and Rothman, J.E. (1993). Binding of coatomer to Golgi membranes requires ADP-ribosylation factor. J. Biol. Chem. 268, 12083–12089.

Presley, J.F., Cole, N.B., Schroer, T.A., Hirschberg, K., Zaal, K.J., and Lippincott-Schwartz, J. (1997). ER-to-Golgi transport visualized in living cells. Nature 389, 81–85.

Reilly, B.A., Kraynack, B.A., VanRheenen, S.M., and Waters, M.G. (2001). Golgi-to-endoplasmic reticulum (ER) retrograde traffic in yeast requires Dsl1p, a component of the ER target site that interacts with a COPI coat subunit. Mol. Biol. Cell 12, 3783–3796.

Saini, D.K., Karunarathne, W.K., Angaswamy, N., Saini, D., Cho, J.H., Kalyanaraman, V., and Gautam, N. (2010). Regulation of Golgi structure and secretion by receptor-induced G protein βγ complex translocation. Proc. Natl. Acad. Sci. USA 107, 11417–11422.

Saitoh, A., Shin, H.W., Yamada, A., Waguri, S., and Nakayama, K. (2009). Three homologous ArfGAPs participate in coat protein I-mediated transport. J. Biol. Chem. 284, 13948–13957.

Scheel, J., Pepperkok, R., Lowe, M., Griffiths, G., and Kreis, T.E. (1997). Dissociation of coatomer from membranes is required for brefeldin A-induced transfer of Golgi enzymes to the endoplasmic reticulum. J. Cell Biol. 137, 319–333.

Schindler, C., Rodriguez, F., Poon, P.P., Singer, R.A., Johnston, G.C., and Spang, A. (2009). The GAP domain and the SNARE, coatomer and cargo interaction region of the ArfGAP2/3 Glo3 are sufficient for Glo3 function. Traffic 10, 1362–1375.

Shiba, Y., and Randazzo, P.A. (2012). ArfGAP1 function in COPI mediated membrane traffic: currently debated models and comparison to other coat-binding ArfGAPs. Histol. Histopathol. 27, 1143–1153.

Shiba, T., Kawasaki, M., Takatsu, H., Nogi, T., Matsugaki, N., Igarashi, N., Suzuki, M., Kato, R., Nakayama, K., and Wakatsuki, S. (2003). Molecular mechanism of membrane recruitment of GGA by ARF in lysosomal protein transport. Nat. Struct. Biol. 10, 386–393.

Shiba, Y., Kametaka, S., Waguri, S., Presley, J.F., and Randazzo, P.A. (2013). ArfGAP3 regulates the transport of cation-independent mannose 6-phosphate receptor in the post-Golgi compartment. Curr. Biol. 23, 1945–1951.

Simpson, J.C., Joggerst, B., Laketa, V., Verissimo, F., Cetin, C., Erfle, H., Bexiga, M.G., Singan, V.R., Hériché, J.K., Neumann, B., et al. (2012).

Genome-wide RNAi screening identifies human proteins with a regulatory function in the early secretory pathway. Nat. Cell Biol. *14*, 764–774.

Söderberg, O., Gullberg, M., Jarvius, M., Ridderstråle, K., Leuchowius, K.J., Jarvius, J., Wester, K., Hydbring, P., Bahram, F., Larsson, L.G., and Landegren, U. (2006). Direct observation of individual endogenous protein complexes in situ by proximity ligation. Nat. Methods *3*, 995–1000.

Stow, J.L., de Almeida, J.B., Narula, N., Holtzman, E.J., Ercolani, L., and Ausiello, D.A. (1991). A heterotrimeric G protein, G alpha i-3, on Golgi membranes regulates the secretion of a heparan sulfate proteoglycan in LLC-PK1 epithelial cells. J. Cell Biol. *114*, 1113–1124.

Weimer, C., Beck, R., Eckert, P., Reckmann, I., Moelleken, J., Brügger, B., and Wieland, F. (2008). Differential roles of ArfGAP1, ArfGAP2, and ArfGAP3 in COPI trafficking. J. Cell Biol. *183*, 725–735.

Weiss, T.S., Chamberlain, C.E., Takeda, T., Lin, P., Hahn, K.M., and Farquhar, M.G. (2001). Galpha i3 binding to calnuc on Golgi membranes in living cells monitored by fluorescence resonance energy transfer of green fluorescent protein fusion proteins. Proc. Natl. Acad. Sci. USA *98*, 14961–14966.

Weller, S.G., Capitani, M., Cao, H., Micaroni, M., Luini, A., Sallese, M., and McNiven, M.A. (2010). Src kinase regulates the integrity and function of the Golgi apparatus via activation of dynamin 2. Proc. Natl. Acad. Sci. USA *107*, 5863–5868.